Final Report • April 1993

OCEANOGRAPHIC DATA PROCESSING PROGRAM

JAMES F. ARNOLD, *Sr. Research Engineer*
SCOTT W. SHAW, *Sr. Research Engineer*
Acoustics and Radar Technology Laboratory

Prepared for:

Office of Naval Research
800 N. Quincy St.
Arlington, VA 22217
Attn: Dr. Joseph Kravitz

Contract N00014-92-C-0015

SRI Project 3047

Approved by:

J. RAUL MARTINEZ, *Director*
Acoustics and Radar Technology Laboratory

TAYLOR W. WASHBURN, *Vice President and Director*
System Technology Division

OFFICE OF THE UNDER SECRETARY OF DEFENSE (ACQUISITION)
DEFENSE TECHNICAL INFORMATION CENTER
CAMERON STATION
ALEXANDRIA, VIRGINIA 22304-6145

IN REPLY REFER TO DTIC-OCC

May 5, 1993

SUBJECT: Distribution Statements on Technical Documents

TO: Office of the Chief of Naval Research
800 North quincy street
Arlington, VA 22217-5000
ATTN: Dr. Joseph n. Kravitz

1. Reference: DoD Directive 5230.24, Distribution Statements on Technical Documents, 18 Mar 87.

2. The Defense Technical Information Center received the enclosed report (referenced below) which is not marked in accordance with the above reference.

Final Report SRI Project ETU-3047
SRI Project ETU-3047
N00014-92-C-0015

3. We request the appropriate distribution statement be assigned and the report returned to DTIC within 5 working days.

4. Approved distribution statements are listed on the reverse of this letter. If you have any questions regarding these statements, call DTIC's Cataloging and Selection Branch (703) 274-6837.

FOR THE ADMINISTRATOR:

Margaret Brautigam

1 Encl

MARGARET BRAUTIGAM
Chief, Cataloging and
Selection Branch

occ file cy

FL-171
Nov 91

DISTRIBUTION STATEMENT A:

APPROVED FOR PUBLIC RELEASE: DISTRIBUTION IS UNLIMITED

DISTRIBUTION STATEMENT B:

DISTRIBUTION AUTHORIZED TO U.S. GOVERNMENT AGENCIES ONLY; (Indicate Reason and Date Below). OTHER REQUESTS FOR THIS DOCUMENT SHALL BE REFERRED TO (Indicate Controlling DoD Office Below).

DISTRIBUTION STATEMENT C:

DISTRIBUTION AUTHORIZED TO U.S. GOVERNMENT AGENCIES AND THEIR CONTRACTORS; (Indicate Reason and Date Below). OTHER REQUESTS FOR THIS DOCUMENT SHALL BE REFERRED TO (Indicate Controlling DoD Office Below).

DISTRIBUTION STATEMENT D:

DISTRIBUTION AUTHORIZED TO DOD AND U.S. DOD CONTRACTORS ONLY; (Indicate Reason and Date Below). OTHER REQUESTS SHALL BE REFERRED TO (Indicate Controlling DoD Office Below).

DISTRIBUTION STATEMENT E:

DISTRIBUTION AUTHORIZED TO DOD COMPONENTS ONLY; (Indicate Reason and Date Below). OTHER REQUESTS SHALL BE REFERRED TO (Indicate Controlling DoD Office Below).

DISTRIBUTION STATEMENT F:

FURTHER DISSEMINATION ONLY AS DIRECTED BY (Indicate Controlling DoD Office and Date Below) or HIGHER DOD AUTHORITY.

DISTRIBUTION STATEMENT X:

DISTRIBUTION AUTHORIZED TO U S GOVERNMENT AGENCIES AND PRIVATE INDIVIDUALS OR ENTERPRISES ELIGIBLE TO OBTAIN EXPORT-CONTROLLED TECHNICAL DATA IN ACCORDANCE WITH DOD DIRECTIVE 5230.25, WITHHOLDING OF UNCLASSIFIED TECHNICAL DATA FROM PUBLIC DISCLOSURE, 6 Nov 1984 (Indicate date of determination) CONTROLLING DOD OFFICE IS (Indicate Controlling DoD Office).

The cited documents has been reviewed by competent authority and the following distribution statement is hereby authorized.

A
(Statement)

UNCLASSIFIED
office report
(Reason)

JOSEPH KRAVITZ
(Signature & Typed Name)

(Assigning Office)

Office that possesses
(Controlling DoD Office Name)

Naval Air Warfare
(Controlling DoD Office Address, City, State, Zip)

5/1/91
(Date Statement Assigned)

CONTENTS

ILLUSTRATIONS

TABLES

1 INTRODUCTION

1.1 Program Overview

The purpose of the FY92/93 effort[1] was to investigate and, where appropriate, develop and deliver software tools to improve the productivity and quality of oceanographic data interpretation. Specifically, this effort comprised three tasks:

- **Task 1: Research and Develop Methods for Improving the Performance of Automated Outlier Detection.** Based on algorithms and software developed by SRI under a previous DMA program,[2] several enhancements were carried out.
- **Task 2: Implement, Document, and Deliver the Improved Outlier Detection Algorithms.** Additional modifications were made to support generic multibeam format (GMF) data sets. The upgraded software was delivered to the hydrographic and bathymetric groups at the Naval Oceanographic Office (NAVOCEANO) and NOAA, and will be delivered to the Defense Mapping Agency (DMA) concurrent with this final report. These improvements are summarized in Section 2.
- **Task 3: Identify and Evaluate More Advanced Oceanographic Data Analysis Tools.** A study was made to determine the data automation needs of the oceanographic community, and then compare these needs to data analysis tools already developed for other scientific application areas. The survey of data automation needs was carried out with the assistance of NAVOCEANO, DMA, and NOAA. Our research indicated that a significant body of relevant techniques has indeed been developed for applications such as robotics, image understanding, and various statistical analysis applications. A summary of our results was presented in our February 1993 technical research memorandum, "Oceanographic Data Processing Feasibility Study" [1].

1.2 Background

In a previous (FY90/91) effort sponsored under the DMA Defense Hydrographic Initiative (DHI), SRI was tasked to develop of a general-purpose outlier detection algorithm for use with multibeam sonar systems. Depth outliers are a particularly common problem in deep-water multibeam sonar systems, and must be eliminated from the data prior to seafloor map production. The time required to manually locate and remove outliers represents a significant portion of the overall data production time and labor. Furthermore, missed outliers can lead to substantial errors in the final map product.

The result of this earlier effort was the development and deployment of a software tool that automates outlier recognition and deletion. Two diverse approaches to outlier detection were developed: the Graduated Non-Convexity (GNC) algorithm, adapted from computer vision

1. 1992/93 contract managed by the Office of Naval Research, Contract N00014-92-C-0015.
2. 1990/91 contract also managed by the Office of Naval Research, Contract N00014-90-C-0132.

applications; and the Robust Linear Prediction (RLP) algorithm, adapted from the field of digital image restoration. Both algorithms were consolidated in a single interactive software package that included an interface to several bathymetry data formats, parameter controls, and graphic displays. Prototype software releases were delivered to the Naval Oceanographic Office (NAVOCEANO), NOAA, and DMA.

The performance of this system was investigated in experiments on U.S. Navy SASS, Seabeam, and Krupp Atlas Hydrosweep bathymetry data sets. An extensive analysis was carried out on a collection of representative SASS data sets by a NAVOCEANO/GBA team. In the NAVOCEANO experiment, the outliers located by the algorithms were compared with those identified by experienced Navy bathymetrists. The automatic outlier detection system located 66% - 85% of valid outliers (where the performance varied somewhat depending on the nature of the test data sets), with false-detection rates of less than 0.03% [2]. These results were considered encouraging by the oceanographic community. The low false-detection rate is especially important, because this loss rate is small in comparison to typical sonar data dropout rates and is believed not to materially alter the final bathymetry product. As a consequence of these results, NAVOCEANO has integrated the outlier detection algorithms into their bathymetric data production process.

These tests also identified high-priority performance improvements for the automated outlier detection algorithms. Specific suggestions were made by groups in the oceanographic community (as reported in Arnold and Shaw [2]), and these form the basis for the algorithm research and development carried out under Task 1 of the current program. An additional requirement to support NAVOCEANO hydrographic data production was recognized, and set forth as Task 2. Finally, a requirement to automate other data interpretation tasks, as called for by the DHI program, is the basis for the feasibility study carried out under Task 3.

1.3 Acknowledgments

As in our previous effort, SRI received technical assistance that proved to be absolutely essential to our work. We would like to thank the staff of NAVOCEANO, and in particular Rich Sandy, who took the time to tutor us in the special needs of bathymetric and hydrographic data production; and Dr. Tom Davis, now of SAIC, for his highly relevant comments and continued support of automation efforts.

2 TASK SUMMARIES

2.1 Task 1: Outlier Detection Algorithm Improvements

Two fundamentally different outlier detection algorithms were considered under this program. The first technique, the graduated non-convexity (GNC) algorithm, reconstructs the ocean floor surface based on a combination of the sonar depth estimates and constraints for surface smoothness and discontinuity. Sonar sample points that significantly differ from the re-estimated surface are identified as potential outliers. The second approach, the robust linear prediction (RLP) algorithm, adaptively develops statistical model parameters from the data set. The expected depth of each sample point is predicted from the values and statistics of the neighboring depth samples. If the actual depth varies significantly from the predicted value, the sample is identified as an outlier and the region is reviewed with the anomalous sample removed.

2.1.1 GNC Algorithm Improvements

The outlier detection properties of the GNC are a side effect of the algorithm's ability to develop a surface with discontinuities: the system has been adapted to recognize very small and hence physically impossible discontinuities as outliers. The computer vision model, unfortunately, does not accurately reflect the true characteristics of the ocean floor, which is typically a continuous (albeit sometimes steep) surface that rarely contains occlusions.

A second point is that the original (FY90/91) GNC algorithm was based on a first-order statistical model for the seafloor. In a first-order model, the depth differences between adjacent points on the seafloor are modeled as a zero-mean, Gaussian random process. Review of statistical studies by Fox [3] indicated that this model is accurate in relatively flat seafloor regimes, but that a second-order model is more appropriate in regions with strong topographic features (Figure 1). This finding corroborates our 1991 experimental evidence that the first-order model had difficulty in steeply sloped regions [2].

From the above, it was determined that the surface energy function used by the GNC should be reformulated to

1. Emphasize singularities (outliers).
2. Incorporate a second-order energy model.

Background on GNC Algorithm. The GNC algorithm is a visible-surface reconstruction technique originally developed for computer vision and three-dimensional mapping systems. In a typical GNC application, such as the simple example of Figure 2, an active range-finder sensor (sonar or an IR ranging device) develops a collection of range estimates over some viewable

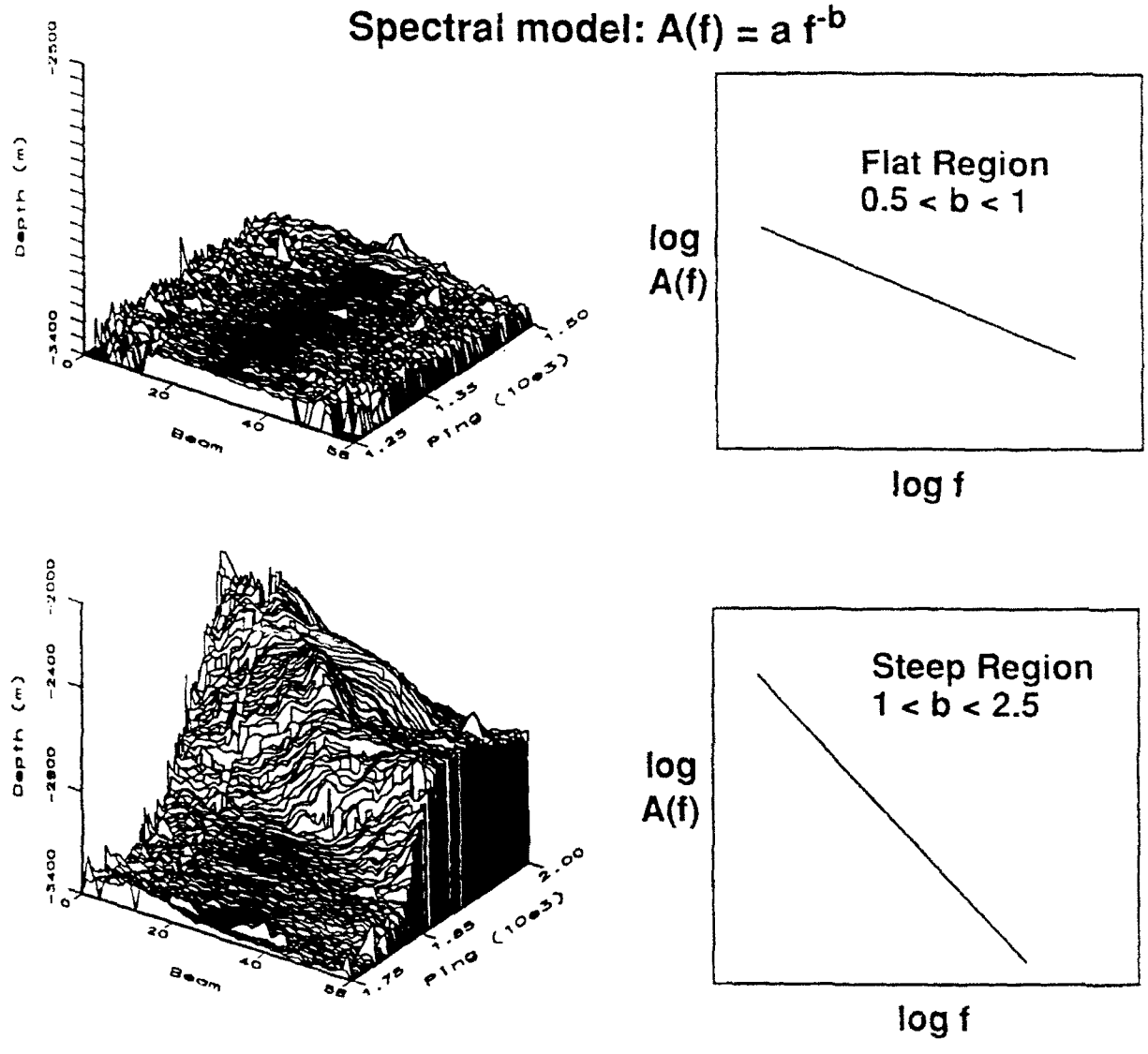

Source: Seafloor spatial statistical model derived from Fox [3]

856-2

FIGURE 1 SPECTRAL MODEL COMPARISON

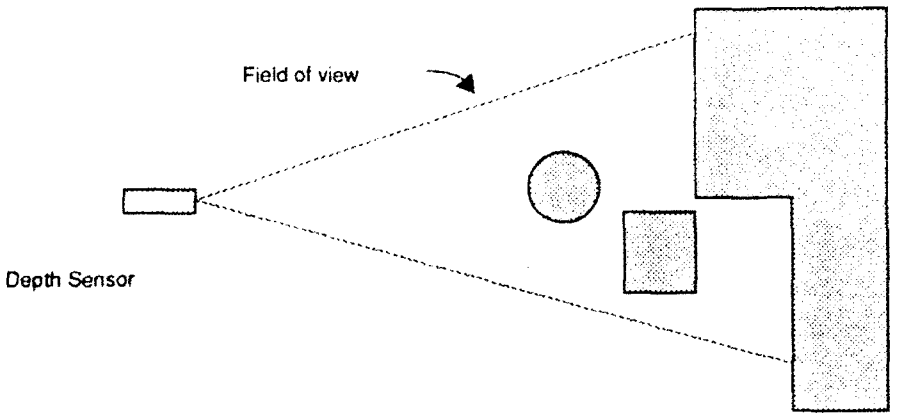

(a) Example Computer Vision Application

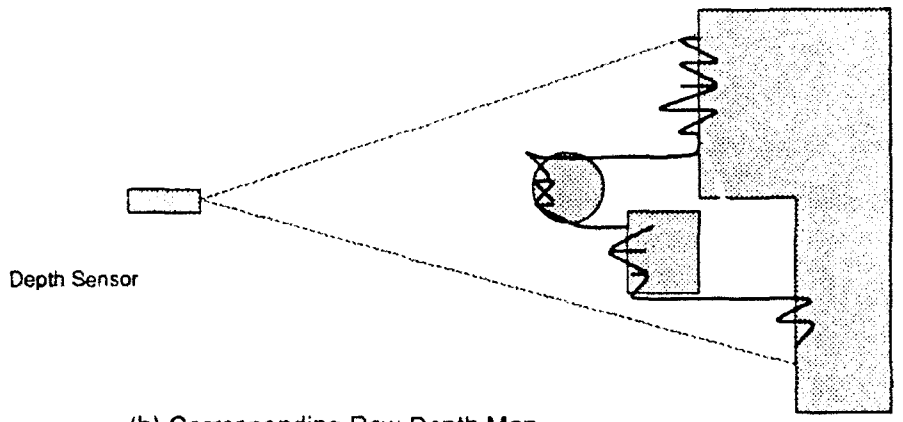

(b) Corresponding Raw Depth Map

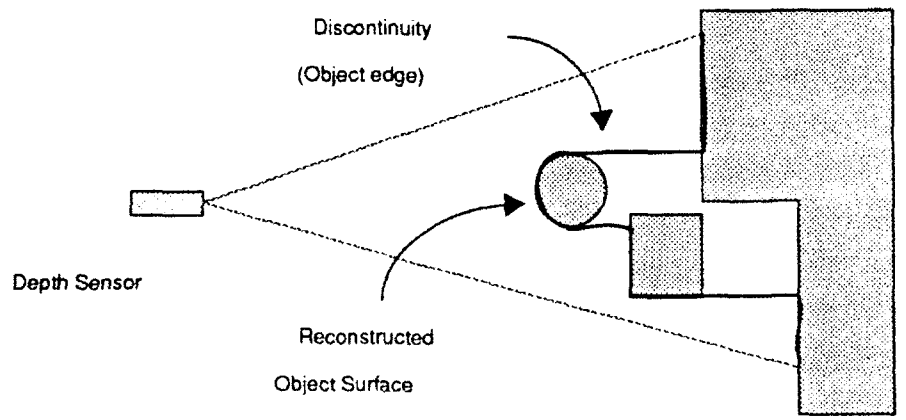

(c) Estimated Visible Surface

FIGURE 2 VISIBLE-SURFACE RECONSTRUCTION

region of interest. After the sensor performs a scan, a potentially noisy discrete depth map is created. The resulting visible surface consists of piecewise continuous regions formed by object surfaces, with discontinuities (i.e., significant jumps in depth) at the object boundaries.

The GNC algorithm is used to estimate the object edge locations, as well as to reduce the noise and thereby improve the shape and position estimates of object surfaces. A combination of factors is used in the surface reconstruction process, including constraints for smoothness (e.g., prior knowledge on the shapes of potential objects), depth discontinuities, and reliability of the measurement data. These competing criteria are quantified in terms of a surface energy function, where the minimum-energy surface represents the most probable solution. The primary technical contribution of the GNC algorithm is the nonlinear optimization procedure by which it locates the minimum-energy configuration.

Surface Energy Models. GNC constrains the estimated surface by applying simultaneous constraints for surface smoothness, continuity, and adherence to the raw sonar data, as quantified through the function $E(u, d)$:

$$E(u, d) = D(u, d) + S(u) + P(u) \tag{1}$$

where

$D(u, d)$ measures adherence of the smoothed surface estimates to the data

$S(u)$ is a surface smoothness function

$P(u)$ is a surface and/or derivative discontinuity function.

The energy model used in the FY90/91 GNC implementation is based on a first-order, or "weak membrane" model. The weak-membrane analogy is a thin rubber sheet that attempts to minimize the vertical slope, but tears if stretched beyond some strength limit. The weak-membrane energy function is calculated as a sum of energy contributions over the entire surface undergoing reconstruction:

$$E_1(u, d) = \sum_{i,j \in S} \left[(u_{i,j} - d_{i,j})^2 + \lambda^2 (1 - L_{i,j}) (u_x^2 + u_y^2) + \alpha L_{i,j} \right] \tag{2}$$

where

$E_1(u, d)$ is the first-order surface energy function

$u_{i,j}$ and $d_{i,j}$ are discrete samples from the reconstructed surface and sonar measurement set, respectively, at each point $\{i, j\}$ on the reconstructed surface, S

λ is a first-order smoothness parameter.

α is the energy associated with surface discontinuities (analogous to the membrane "strength").

u_x and u_y are the x and y spatial first derivatives at each point $\{i, j\}$.

$L_{i,j}$ is a discontinuity indicator, such that:

$$L_{i,j} = \begin{cases} 1 \text{ at discontinuities} \\ 0 \text{ elsewhere} \end{cases}$$

The variable $L_{i,j}$ enables surface discontinuities that are key to this application; at points where $L_{i,j} = 1$, the smoothness constraint is ignored and a fixed energy, α, is assigned. At all other points, the smoothness energy, $\lambda^2 (u_x^2 + u_y^2)$, is assessed. The relative value of the smoothness parameter, λ, and the discontinuity energy, α, determine the algorithm's proclivity toward discontinuities.

A second-order, or thin plate, model was developed under the 1992/93 effort. The second-order approach provides surface-fitting behavior like that of a stiff but deformable plate. As inferred from the thin-plate analogy, this model favors surfaces with constant slopes, while resisting strong surface curvature. The surface is allowed to break, however, causing discontinuities in the surface and its first derivative. The thin-plate-model energy function used in this effort[3] is given as

$$E_2(u, d) = \sum_{i,j \in S} \left[(u_{i,j} - d_{i,j})^2 + \mu^4 (1 - L_{i,j}) (u_{xx}^2 + u_{yy}^2) + \alpha L_{i,j} \right] \tag{3}$$

where

$E_2(u, d)$ is the second-order surface energy function

μ is the second order smoothness parameter

α is the energy associated with surface discontinuities

u_{xx} and u_{yy} are the second-order spatial derivatives at points $\{i, j\}$

$L_{i,j}$ is the discontinuity indicator.

Surface Energy Minimization. Reliable minimization of the energy function, $E(u, d)$, requires a complete search over all possible reconstructed ocean depths, $u_{i,j}$, for all points on the surface. In most applications, and in particular bathymetric, such searches are intractable because of the extremely large number of possible surfaces. Alternatively, if the locations of the discontinuities, $L_{i,j}$, are fixed, the minimization can be posed as a common linear least-squares problem. In this

3. Other second-order energy functions are also possible; for example, a reasonable function might account for both first- and second-order smoothness, and/or rely on the derivative crossterms u_{xy} and u_{yx}.

case, a least-squares solution to $u_{i,j}$ would be found for all possible collections of discontinuities, and the discontinuity set providing the minimum-energy surface would be chosen. This may be a plausible approach if the number of expected ocean floor discontinuities is small. The processing requirements quickly grow unmanageable, however, because the number of feasible outlier configurations grows combinatorially with the number of possible outliers.

Blake and Zisserman proposed the GNC as a practical solution for problems of this kind [4]. The primary contribution of the GNC algorithm is the unique method by which it carries out the energy minimization process. Rather than minimize the energy function directly (e.g., through an exhaustive search), the algorithm forms a bounded approximating function with special convexity properties. Once the minimum of the approximating (convex) function is located, a more accurate approximating function is created and the minimization process is repeated. The accuracy of the energy-minimum estimate is refined as the approximating function approaches the true energy function.

For notational convenience, the smoothness and discontinuity contributions of the energy function are usually consolidated, forming the energy function

$$F = D + \Sigma [\, g(u_{xx}) + g(u_{yy}) \,], \tag{4}$$

where D is the measurement adherence function, and $g(t)$ contains both the smoothness and discontinuity functions. In the case of the second-order model, $g(t)$ is given by

$$g(t) \equiv \mu^2 (1 - L_{i,j})\, t^2 + \alpha L_{i,j}. \tag{5}$$

Blake and Zisserman have shown [4] that the best-fit convex approximation to $g(t)$ is

$$g^{(p)}(t) = \begin{cases} \mu^4 t^2 & \text{for } (t < q) \\ \alpha - c\,\dfrac{(t-r)^2}{2} & \text{for } (q \le t < r) \\ \alpha & \text{for } (t \ge r) \end{cases}$$

where

$$c = \frac{c^*}{p}, \qquad r^2 = \alpha \left(\frac{2}{c} + \frac{1}{\mu^4}\right), \qquad q = \frac{\alpha}{r\mu^4} \tag{6}$$

and t is the second derivative about the depth sample. The function $g^{(p)}$ takes any of three forms, depending on the value of the argument. For small depth differences, the magnitude of t is small and the smoothness energy criteria, $\mu^4 t^2$, applies. Large depth differences represent discontinuities, and the discontinuity energy, α, is assessed. In both the small- and large-difference cases, the

approximating function is exact. At intermediate depth differences, a quadratic (and hence convex) approximation is used.

The parameter p controls the energy function approximation. The algorithm locates the solution iteratively, beginning with $p = 1$, such that $g^{(1)} = g^*$ and the approximating energy function is globally convex. After a solution for $g^{(1)}$ is located, p is decreased and a new (more accurate) solution is found. As the algorithm proceeds, p is slowly decreased toward zero and a refined estimate is calculated at each point. Note that at $p = 0$, the approximating energy function is precise, and the true energy minimum is located. The algorithm's operation is summarized in Table 1.

Table 1. SECOND-ORDER GNC ALGORITHM SUMMARY

Initialize:

for i = 1, ... N_i , j = 1, ... N_j

$$u^0_{i,j} = d$$

Reconstruct:

for p = 1, 1/2, 1/4, ...

for n = 1, ... N (iterations on the reconstructed image)

for i = 1, ... N_i j = 1 ... N_j

$$u^{n+1}_{i,j} = u^n_{i,j} + \gamma\left((u^n_{i,j} - d_{i,j}) + g^{(p)}\,(u^{xx}_{i,j}) + g^{(p)}\,(u^{yy}_{i,j}) \right)$$

where $u^{xx}_{i,j}$ and $u^{yy}_{i,j}$ are the second derivatives with respect to depth in the x and y dimensions, respectively, of the reconstructed seafloor surface, u, at iteration interval n; $d_{i,j}$ is the raw depth sample at position $\{i,j\}$; and γ is the adaptation gain constant.

Empirical Comparison of First- and Second-Order Models. Seafloor reconstruction results obtained with the first- and second-order GNC algorithms are given in Figure 3. The test data set was excerpted from a 1990 University of Rhode Island Hydrosweep cruise of the North Atlantic near 64° latitude, 5° longitude. As shown in the three-dimensional plot of Figure 3a, the selected data set contains a significant topographic feature. Results from the first-order GNC algorithm (Eq. [3]) are shown in Figure 3b. Note that the first-order reconstructed surface has linear tears following across the steeply sloped regions, causing the reconstructed surface to differ greatly from the underlying data. True outliers in the steep regions are masked by these tears, thereby reducing the outlier detection effectiveness.

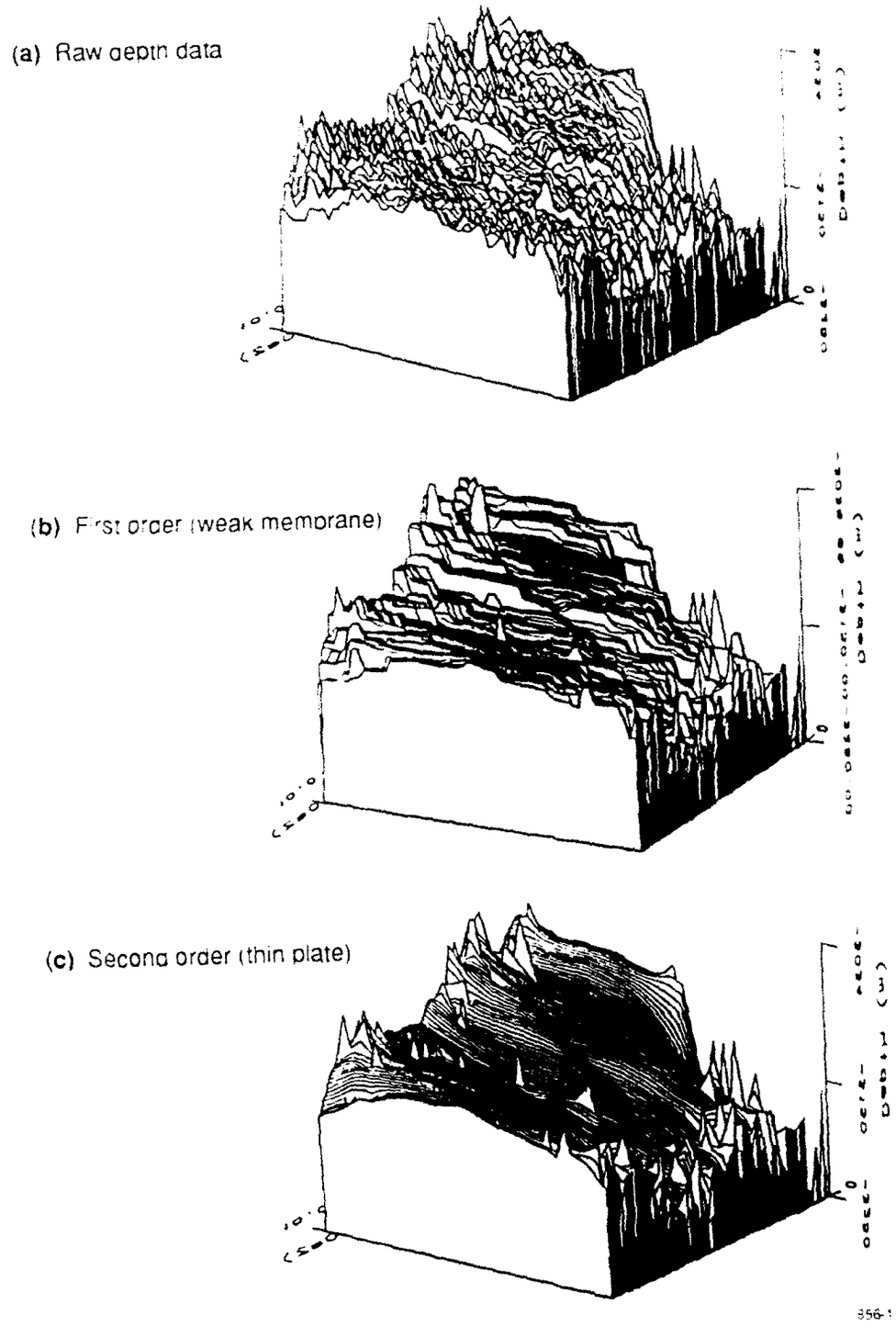

FIGURE 3 FIRST- VS. SECOND-ORDER RECONSTRUCTION

The second-order, or thin-plate reconstruction (Eq. [4]) results are shown in Figure 3c. Because the second-order model is a better match to this data set, the reconstructed surface is continuous through steep regions, yet identifies breaks in the surface to accommodate outliers. Several outliers are present, however, in the form of occasional spikes in the data.

2.1.2 RLP Algorithm Improvements

The RLP algorithm operates by

1. Estimating autoregressive parameters for some window of data.
2. Predicting depth at a beam-ping bin based on the estimated parameters and some neighborhood of surrounding bins.
3. Comparing the predicted depth to the measured depth at that bin and making some decision.

Rather than being arbitrary, the shape of the prediction neighborhood is governed by the mathematics of the parameter estimation procedure. To simplify this procedure, we followed standard, image-processing procedure and employed a nonsymmetric prediction neighborhood. Unfortunately, this choice has unwanted side effects, including:

- Probability of outlier detection depends on the direction of filtering, whether from early times to later times, or vice versa.
- Because of the one-sided prediction, the RLP tends to produce false alarms at transition zones.

Improvements to the RLP algorithm were designed to overcome the directionality of the nonsymmetric-half-plane support region and to lower the false-alarm rate on steeply dipping regions.

Background on RLP Algorithm. The RLP algorithm characterizes outliers as samples of a non-Gaussian random process. The tools of robust estimation theory allow us to detect these samples without assuming a parametric form of the outlier probability density. The RLP algorithm operates adaptively by robustly estimating the parameters of an autoregressive (AR) ocean bottom process within some small window, and then using these parameters to predict depths within the same window. The estimation window steps across a few beams and pings at a time, as shown in Figure 4. If a measured depth exceeds some threshold, it is replaced by its predicted value and the estimation process repeats. Outliers are declared when the difference between the restored surface and the original surface exceeds some threshold. This approach offers several benefits:

- The ocean bottom is modeled accurately, even in the presence of large sensor errors.
- What is known (the ocean bottom statistics) is exploited, and what is unknown (the outlier statistics) is removed.

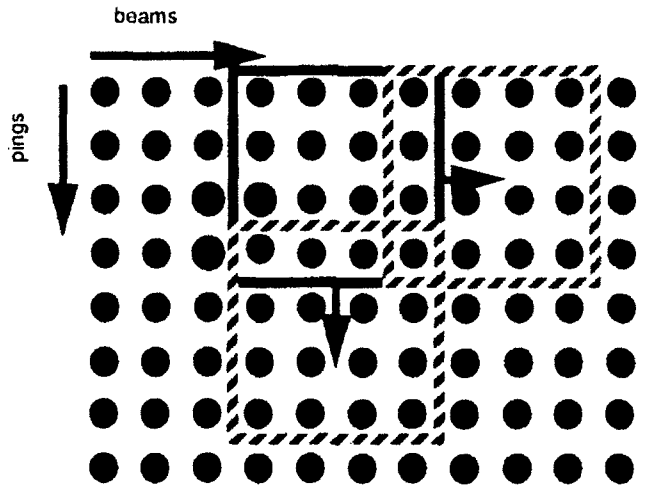

FIGURE 4 MOVEMENT OF ESTIMATION WINDOW ACROSS DATA SET IN OVERLAPPING STEPS

- The process adapts to the local ocean bottom statistics without reliance on a global surface estimate.
- Ocean bottom discontinuities are modeled and not reported as outliers.
- Allowance is made for random sampling errors (beam-ping format data).

Robust Bathymetric Error Detection. The RLP algorithm was adapted from an image restoration algorithm reported by Kashyap and Eom [5]. In this technique, a robust M-estimator is used to estimate the parameters of an autoregressive image model. These parameters are then used in a "data cleaning" step, where outliers are removed. The AR parameters are again estimated and the data cleaned, and so on, until no more outliers are found.

The Kashyap algorithm assumes a first-order, nonsymmetric half-plane (NSHP) image model. This model is the two-dimensional equivalent of a causal model in time series analysis (Figure 5). In the NSHP model, an intensity, $y(i,j)$, is computed as the weighted sum of the three "neighbors" shown in Figure 5, plus some random innovation. If θ_k is the weight given to the k^{th} neighbor of point (i,j), this relation may be written

$$y(i,j) = \theta_1 y(i-1,j) + \theta_2 y(i-1,j-1) + \theta_3 y(i,j-1) + \upsilon(i,j),$$

where $\upsilon(i,j)$ is a zero-mean Gaussian random field with variance σ_υ^2. In vector notation, this would be written

$$y(i,j) = \underline{\theta}^t \underline{z}(i,j) + \upsilon(i,j), \tag{7}$$

where $z(i,j)$ is a 3x1 vector of NSHP neighbor values surrounding point (i,j). The image is further assumed to be contaminated by some unknown outlier process, $\zeta(i,j)$, whose probability distribution is unknown. Thus, the observed image, $y_o(i,j)$, may be expressed as

$$y_o(i,j) = \theta^t z(i,j) + \upsilon(i,j) + \zeta(i,j) .$$

Given this observation model, a robust M-estimator for the parameters θ and the variance σ_v^2 is found by minimizing the nonlinear expression

$$e = \sum_{i,j} \rho\left(\frac{(y_o(i,j) - \theta^t z_o(i,j))}{\sigma_v} \right).$$

The data-cleaning procedure takes the process further by replacing outliers in each step with the value predicted by the robustly estimated parameters $\hat{\theta}$. Upon convergence, the window is shifted over a few rows or columns and the process repeated. In this way, the entire image is restored, one window at a time.

RLP Modifications. Throughout development of the RLP algorithm, we have relied on a first-order nonsymmetric half-plane image model, which has proven sufficiently flexible to model a variety of ocean bottom processes. It also has the advantage of being recursive, so that missing data points may be estimated as the filter progresses. The NSHP model also has several disadvantages. It has strong directional preferences, and only detects errors on the leading edge of a group

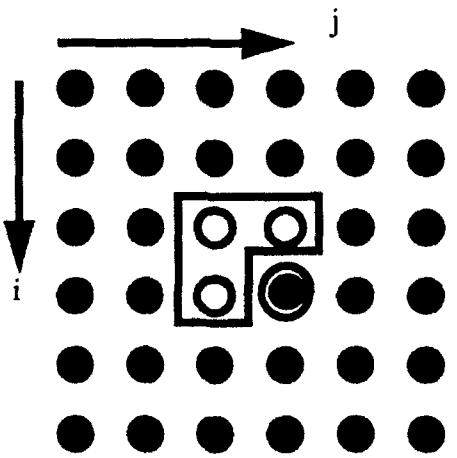

FIGURE 5 NSHP MODEL: UNFILLED POINTS COMPOSE THE NEIGHBORHOOD OF THE CIRCLED POINT.

of error points. This directionality problem may be solved through the use of noncausal error filters.

A more serious drawback of the NSHP model is that it does not reflect the nature of the multibeam bathymetry process. In other words, the elements of the vector $z(i, j)$ in Eq. (7) do not correspond to beams, pings, or any physical entity other than an arbitrary neighborhood of points. This lack of correspondence makes impossible the incorporation of *a priori* information, such as beam or ping confidence measures. The utility of the RLP has been improved by reformulating the surface model to be oriented specifically to multibeam bathymetry. In this algorithm, which we refer to as the vector robust linear prediction (VRLP) algorithm, beam data can be expressed as a vector, Markov random process by replacing Eq. (2) with

$$\underline{p}(t) = \sum_{i=1}^{N} \Theta_i \underline{p}(t-i) + \underline{\nu}(t)$$

where $\underline{p}(t)$ is a length n vector of measurements from a ping at time t, one component for each beam. The parameters of this model are contained in Θ_i, an $n \times n$ matrix, and $\underline{\nu}(t)$ is a vector random process with covariance matrix C. The estimated covariance matrix $\hat{C}$ for such a model now conveys much more information than the covariance, $\hat{\sigma}$, of the scalar NSHP model used previously. For example, the diagonal of $\hat{C}$ contains estimates of the variance of individual beams. If a single element along the diagonal grows much larger than the other elements, an operator can be alerted to the presence of a bad beam.

Rather than directly copy the Kashyap algorithm, we have adopted a vector version of the robust filter-cleaner approach of Martin and Thomson [6]. This algorithm is identical to the Kashyap approach with the exception that simple least-squares estimates (which we obtain by solving vector version of the Yule-Walker equations [7]) of the parameters and covariance are computed at each iteration rather than taking a nonlinear Gauss-Newton step. The data cleaning proceeds as before, with certain modifications for the vector quantities involved.

To improve false-alarm rates on steep slopes, we have further modified the algorithm to perform smoothing rather than filtering. In other words, two models, one forward and one backward, are assumed, and a weighted sum of each is used. This is shown graphically in Figure 6. The models may be written

$$\underline{p}^f_j = \sum_{i=1}^{N_f} \Theta^f_{i,k} \underline{p}^f_{(j-i)} + \underline{\vartheta}^f_j$$

and

$$\underline{p}_j^b = \sum_{i=1}^{N_b} \Theta_{i,k}^b \underline{p}_{(j+i)}^b + \underline{\vartheta}_j^b,$$

where $\underline{\vartheta}_j^f$ and $\underline{\vartheta}_j^b$ are vector random processes with covariance matrices C^f and C^b, respectively. The complete VRLP algorithm is given in Table 2.

Table 2. VECTOR ROBUST LINEAR PREDICTION ALGORITHM

1. $k = 0$

2. Until no change in $\underline{\theta}$ or σ ,
   do

   2.a Using data within the estimation window, compute $\hat{\Theta}_{i,k}^f$, $\hat{\Theta}_{i,k}^b$, $\hat{C}_{i,k}^f$, and $\hat{C}_{i,k}^b$, $i = 1, \ldots, N$, by solving the forward-backward, vector, Yule-Walker equations.

   2.b Perform data cleaning:
   For each ping j in the estimation window,
   do

   2.b.i $$\underline{\hat{p}}_{j,k+1}^f = \sum_{i=1}^{N} \hat{\Theta}_{i,k}^f \underline{\hat{p}}_{(j-i),k}^f + C_f \underline{\Psi}\left[C_f^{-1}\left(\underline{\hat{p}}_{j,k}^f - \sum_{i=1}^{N} \hat{\Theta}_{i,k}^f \underline{\hat{p}}_{(j-i),k}^f \right)\right]$$

   2.b.ii $$\underline{\hat{p}}_{j,k+1}^b = \sum_{i=1}^{N} \hat{\Theta}_{i,k}^b \underline{\hat{p}}_{(j-i),k}^b + C_b \underline{\Psi}\left[C_b^{-1}\left(\underline{\hat{p}}_{j,k}^b - \sum_{i=1}^{N} \hat{\Theta}_{i,k}^b \underline{\hat{p}}_{(j-i),k}^b \right)\right]$$

   2.b.iii $$\underline{\hat{p}}_{j,k+1} = (C_f^{-1} + C_b^{-1})^{-1} (C_f^{-1} \underline{\hat{p}}_{j,k+1}^f + C_b^{-1} \underline{\hat{p}}_{j,k+1}^b)$$

   end

end

   2.c $k = k + 1$

RLP Results. A comparison of the RLP and VRLP algorithms is shown in Figure 7. Figure 7a shows a raw data swath with a variety of errors. Figure 7b shows the results of applying the RLP algorithm to these data. Note that several false alarms are found on the steeply sloping region, and that some outliers are missed on the edges and in the vicinity of a bad beam. Figure 7c shows the results of applying the VRLP algorithm. Note that the number of false alarms is reduced, and that more outliers are detected on the edges and in the middle.

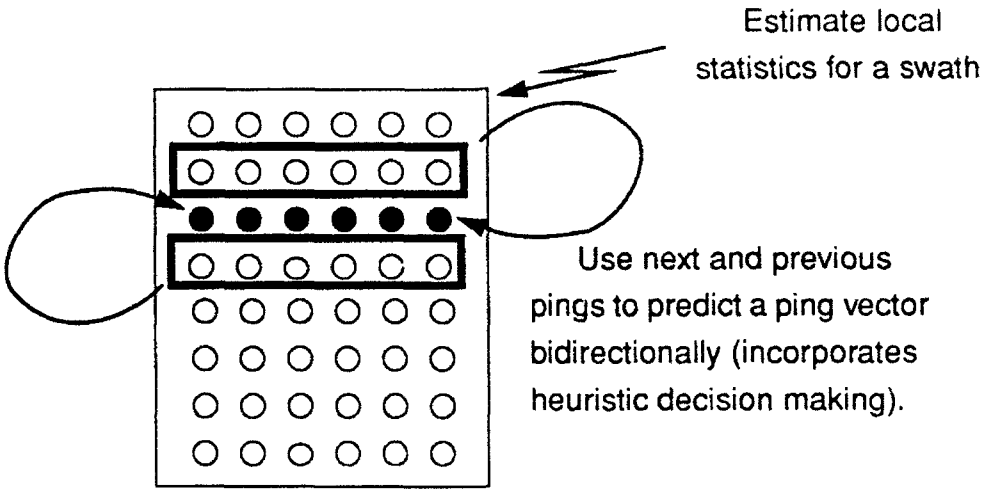

FIGURE 6 BIDIRECTIONAL VRLP ALGORITHM

2.2 Task 2: Outlier Detection Software Implementation and Delivery

2.2.1 Background

The purpose of the *clean* program is to automatically analyze raw depth files produced by bathymetric and hydrographic sensors, and tag the isolated outlier depth estimates in the data. The application environment for *clean* is summarized in Figure 8, where *clean* represents the first step in a four-step bathymetric chart production process. In the second step of Figure 8, the positional information attached to the depth estimates is adjusted to account for navigational errors. The third step calculates and assigns statistical information to the data, such as data reliability indicators and expected errors (in position and/or depth). The fourth and final step combines the individual swaths of depth estimates to form a fully populated, two-dimensional depth grid.

Clean can be applied either as a stand-alone prefilter of sensor data, or used in conjunction with the NAVOCEANO *swathedt* contour display program to provide a semiautomated oceanographic data quality analysis and editing environment. The auxiliary program *control* provides an X-Windows interface to the *clean* processing parameters.

2.2.2 System Operation

A top-level system control and data flow diagram, drawn from the operator's perspective, is shown in Figure 9. Input to the system consists of raw sensor depth files in one of the following formats:

(a) Raw Data

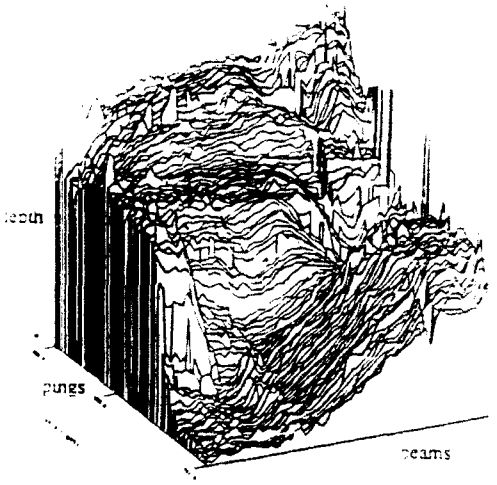

(b) Results of RLP Algorithm

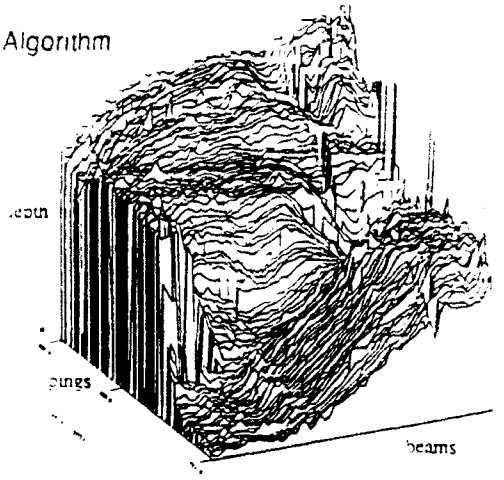

(c) Results of VRLP Algorithm

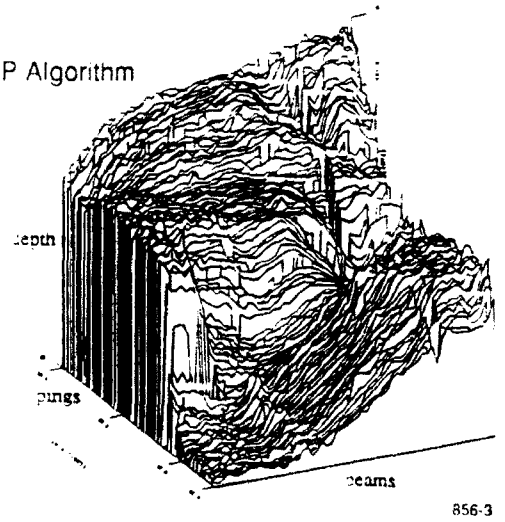

FIGURE 7 RESULTS OF RLP AND VRLP ALGORITHMS

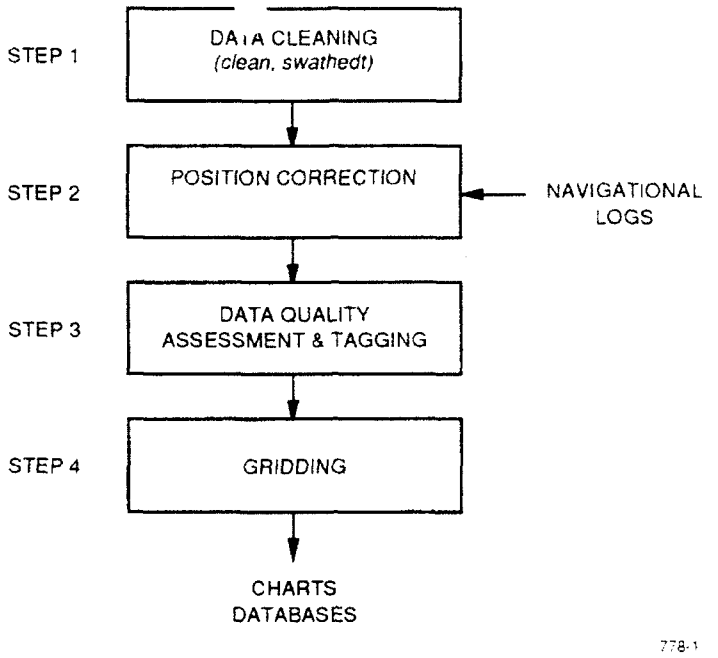

FIGURE 8 APPLICATION ENVIRONMENT: BATHYMETRIC/ HYDROGRAPHIC CHART PRODUCTION

- Compressed SASS and Seabeam
- Uncompressed Seabeam
- Hydrosweep
- Generic multibeam format (GMF).

Clean optionally produces two types of output files:

- Filtered Time Anomaly File (FTAF)
- Edited sensor depth file.

The FTAF is an ASCII file containing the times and beam numbers of detected outliers. Other software, including the *swathedt* contouring program, makes use of the FTAF to graphically highlight outliers. The edited sensor data file has identical format to that of the input file, except that the automatically detected outlier depths have been marked.

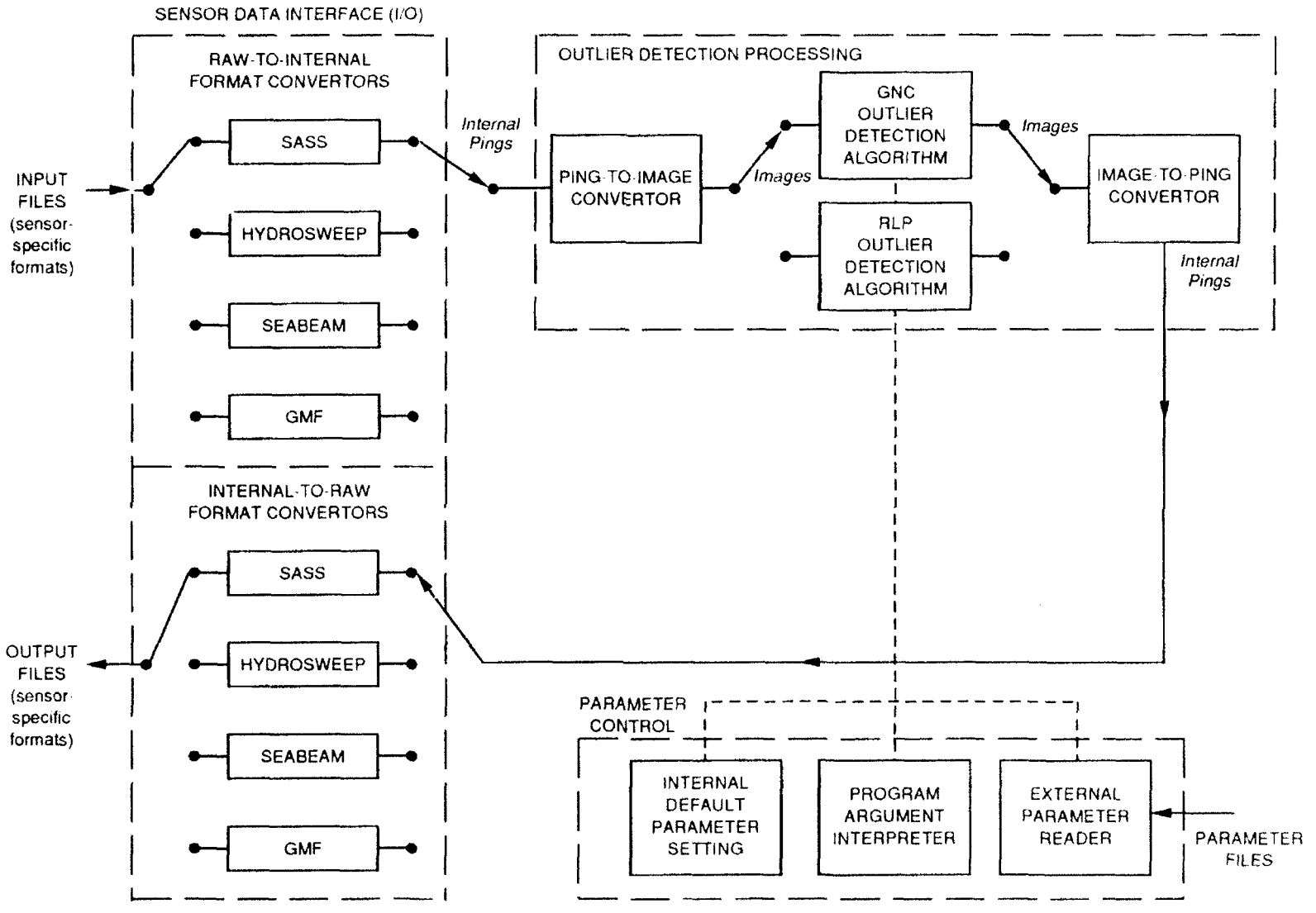

FIGURE 9 *CLEAN* SOFTWARE BLOCK DIAGRAM

Clean is a batch program; once started, it does not require operator interaction. At the start of execution, *clean* is assigned processing parameters that include:

- Input file name (required)
- FTAF file name (optional; if omitted, no FTAF created)
- Range of pings and beams to process (optional; if omitted, all pings & beams processed)
- Outlier detection algorithm parameters (optional; default values used otherwise).

Processing continues until either the operator aborts the run (by explicitly killing the process via an operating system command, e.g., the Unix kill command), or until the specified range of pings is completely processed.

The auxiliary program *control*, an X-windows interface, enables more convenient viewing and editing of the parameters than is possible through standard Unix command-line parameter passing. In addition, *control* allows entire sets of parameters to be saved and recalled using operator-selected names. The parameter values selected in the *control* window are communicated to *clean* via a parameter database file that is shared between the two programs. An example *control* screen image is shown in Figure 10.

2.2.3 Computing Requirements

Clean was designed to operate on any Unix computing system, and to be readily portable (that is, transferable with minimum effort) to other operating systems.Because *clean* is a computationally intensive program, a computer with fast floating-point performance is recommended. *Clean* does not require interactive or graphics support software. The auxiliary program *control*, however, requires a graphics display terminal with keyboard and mouse, along with an X-Windows server and window manager. The details of *control*'s appearance depend on the window manager and the local shareable libraries supporting X. *Control* was implemented under the MOTIF widget set.

Both *clean* and *control* are written in the ANSI/C language, and compile and operate under either the System V (HPUX), BSD4.2, or BSD4.3 versions of the Unix operating system.

2.2.4 Current Status

Version v2.3 of the *clean* and *control* software and their corresponding documentation sets were delivered to NAVOCEANO in June of 1992. On-site software training was provided to NAVOCEANO personnel at that time. The *clean/control* software and User's Guide were also delivered, at DMA's request, to a NOAA facility.

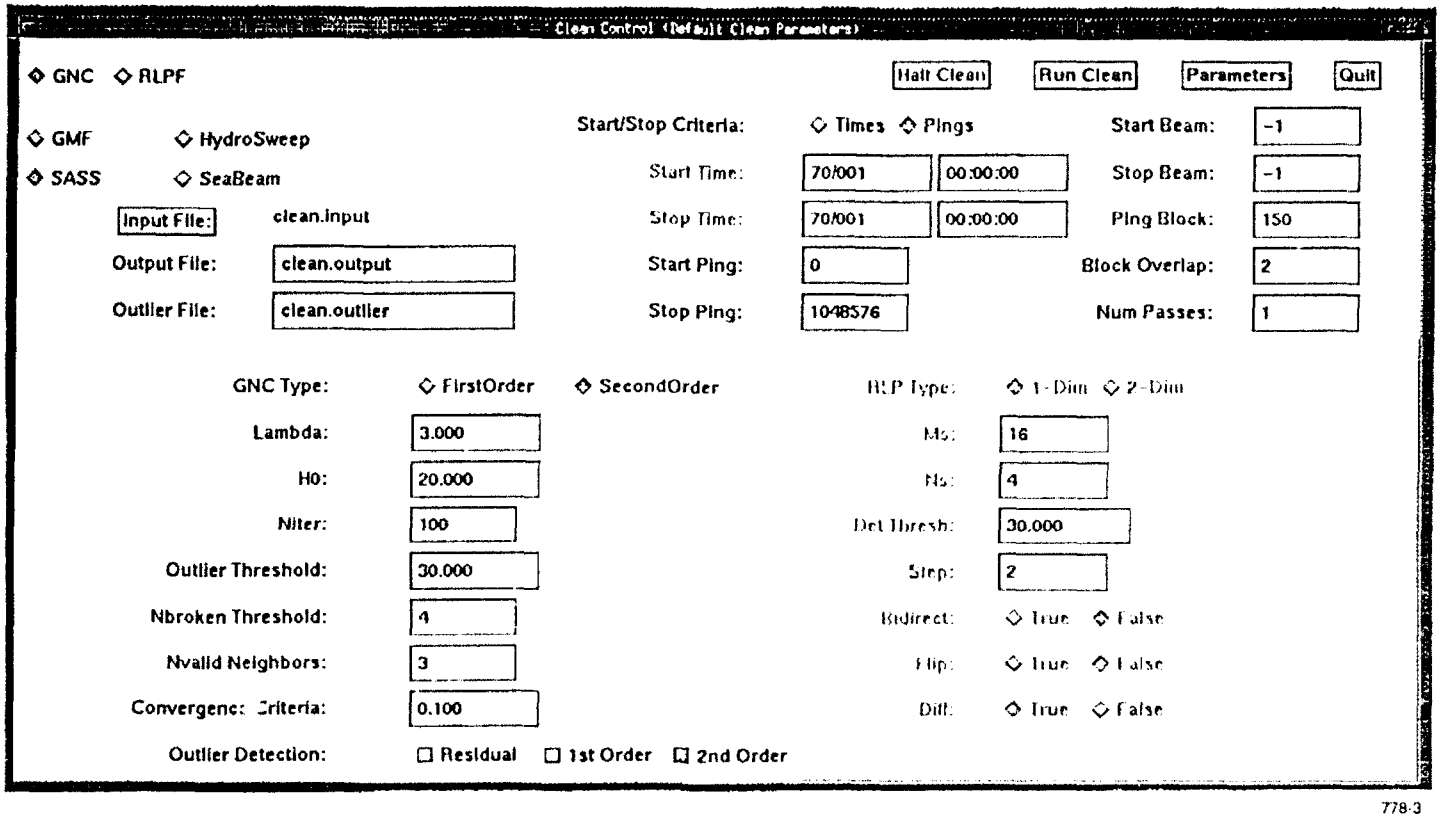

FIGURE 10 *CLEAN* CONTROL PANEL

Items delivered under this task include the software source code, functional system and subsystem descriptions [8,9], and User's Guide [10]. The final software release will be sent to DMA at project completion, circa 1 May 93.

2.3 Task 3: Feasibility Study

In this task, SRI conducted a study to identify data processing techniques already in use for other scientific applications that could be cost-effectively adapted to oceanography. Wherever possible, estimates were made for the additional required R&D, implementation time/cost and technical risk for adapting such techniques to bathymetric/hydrographic data processing problems. In the particular area of error reduction through sonar signal processing improvements, a prototype algorithm was implemented and tested.

The techniques covered in the feasibility study fell roughly into two categories. High-level data processing techniques, which are largely based on methods of computer vision and artificial intelligence, were considered for the problems of bathymetric data fusion, seafloor classification/provincing, and three-dimensional shape and object recognition. Lower-level processing techniques, which are based on methods of statistics and mathematical optimization, were studied for application to *post facto* survey navigation correction, sonar error reduction, and interferometric sidescan sonar processing.

A complete report on our findings was given in "Oceanographic Data Processing Feasibility Study" [1], which was delivered to DMA in February 1993. The following sections summarize our findings for each of the application areas. Recommendations for additional work in these areas are given in Section 3.

2.3.1 Ocean-Bottom Classification/Provincing

This portion of the study considered methods for automatically segregating the ocean floor into regions that are similar in some regard. Typical provincing criteria include bottom composition, roughness, slope, or some particular geological feature. Even if humans are still used to provide the final interpretation, an automatic or semiautomatic provincing capability would be expected to save analysis time. For example, in geophysical studies, the data analysts's job would be greatly simplified if regions of similar topology were identified in advance by the computer. Provincing may also be used to automatically select outlier detection parameters, and recent findings by the DMA Data Integration Working Group (DIWG) indicate that provincing will be required to delineate seafloor regions and automatically select appropriate gridding and interpolation algorithms. Provincing capabilities of this type would also be useful to the ocean

engineering community, where tasks such as cable routing could be simplified if bathymetric provinces were automatically delineated and classified.

The bathymetric classification problem has similarities to problems that have already been addressed in other fields. For example, computer vision techniques are currently used to perform such tasks as characterizing topographies or assessing crop yields from digital terrain maps. In manufacturing applications, computer vision techniques provide real-time assembly-line inspection and quality control. Such techniques are well understood, and could be transferred to oceanographic applications in a relatively short time.

2.3.2 Three-Dimensional Shape Recognition

A general three-dimensional shape recognition capability is a prerequisite to several automatic tasks, including macroscopic error detection (e.g., identifying biases in the sensor estimates), navigational hazard detection, and recognition of topographic features.

As in the case of classification and provincing, a great deal of research has already been conducted on terrestrial map interpretation, as well as on parts identification and fault detection in manufacturing applications. Although a variety of algorithms have been developed to address the three-dimensional shape recognition problem, they rely almost universally on the differential geometric concepts of Gaussian and total curvature. Scale also plays an important role in the shape recognition process, indicating that bathymetric shape analysis algorithms will be required to extract curvature features over scale.

2.3.3 Data Fusion

Data fusion is the process of combining information from multiple sensors to produce composite data that are either more accurate or more reliable than what can be derived from any sensor alone. In bathymetric applications, the candidate sensor types include single- and multibeam sonars, sidescan sonars, and gravity and magnetic sensors. Fusion may take place at low or high levels of data abstraction. For example, depth data from an overlapping set of sonar surveys may be combined at the raw depth-estimate level. Techniques for combining these data are well-known and relatively straightforward to implement; however, combining data from sensors that measure very different phenomena (e.g., magnetic and depth data) is much more difficult. In most cases, features or underlying interpretations must be extracted from each sensor's data stream prior to fusion.

An initial practical goal would be to develop a low-level fusion system that combines two or more bathymetric surveys into a single map product. Such a system could be developed at

relatively low cost, and with little technical risk. The development of a navigational correction algorithm would be a prerequisite to this effort. Additional research will be required, however, before a high-level fusion system can be developed. In particular, knowledge representations must be identified to support specific oceanographic fusion problems and sensor types.

2.3.4 Error Reduction Through Improved Sonar Signal Processing

The signal processing and bottom estimation algorithms currently used in bathymetric sonar systems are subject to outlier errors under a number of common conditions. Sonar beam sidelobes, external interferers, and poor bottom reflectivity can greatly affect system accuracy, leading to such well-known problems as "tunneling," "omega" effects, phantom features, and isolated outliers. While some of these errors can be detected in postanalysis, many are insidious and are easily missed by an analyst. And when such errors are detected, depth data in the affected region are unrecoverable, and the area must be resurveyed or eliminated from the resulting data products.

de Moustier and Kleinrock [11] pointed out that the signal due to the acoustic return from the seafloor is generally still present in the data, but a much stronger signal at an incorrect apparent time-delay confuses the depth estimation algorithms. It is believed that sophisticated depth estimation techniques could make sonar systems much more robust against such problems by comparing the shape and spatial spectra of the seafloor vs. those caused by various error effects, as well as the amplitude characteristics of actual and error signals.

The problem of robust detection and estimation has already been faced in several other application areas. In the field of robotics, surface reconstruction algorithms have been developed to estimate visible surfaces from range measurements that are very similar to those produced by bathymetric sonars. Such approaches rely on a combination of surface shape and consistency constraints to identify likely surface interpretations. The target tracking algorithms used in radar systems address the robustness problem through use of a multiple hypothesis (MH) approach, in which several candidate target tracks (or, in a bathymetric application, several candidate seafloors) are developed and evaluated in parallel. The final selection is delayed until after sufficient supporting data have been analyzed. The MH approach is particularly useful for applications in which sensor errors are not always immediately obvious, such as in the cases of tunneling and omega errors in a multibeam survey.

A prototype depth estimation procedure was developed and briefly tested under this study. The prototype combines a multiple hypothesis procedure with a surface reconstruction algorithm that was derived from the computer vision literature (e.g., Amini et al. [12,13]). Preliminary

experimental results using synthesized depth data[4] have been encouraging, although additional tests on collected sonar data will be required to thoroughly prove the concept.

2.3.5 Automated Navigational Correction

Prior to the introduction of the Global Positioning System (GPS), navigational errors were the predominant source of uncertainty in bathymetric surveys. Unfortunately, most of the existing bathymetric database was created in the pre-GPS era, and many of those surveys contain ship position errors of up to several kilometers. While most bathymetric map production facilities allow navigational corrections, such procedures are manual and time-consuming. In addition, bathymetric data must sometimes be discarded when surveys overlap but do not precisely align, because there is no low-level fusion capability that accounts for the navigation errors and the resulting disagreement in depths. For these reasons, the bathymetrists interviewed under this effort indicated great interest in an automatic, postsurvey navigational correction capability. A similar capability for verifying (but not attempting to correct) the navigation of coastline surveys was also requested by hydrographers.

A search of the open technical literature found that at least two prior researchers developed *postfacto* navigation correction techniques [15-17]. In both techniques, the seafloor topography is used as an alignment feature at points where the survey track passes over itself or over an independent (and possibly more accurate) survey. These approaches reduce the relative position errors that occur over the period of the survey, and if the navigation errors are at least partially uncorrelated, the absolute position errors are reduced as well. More importantly, if two or more survey points are precisely known (e.g., through GPS fixes, or when a survey track overlaps a separate, GPS-navigated survey), the adjusted positional accuracy of the entire track can approach that of a completely GPS-navigated survey.

Based on the results of previous research in this area, we conclude that a postsurvey navigation system is practical. However, before such a system can be used routinely at an oceanographic map-production facility, several problem areas will have to be addressed, including: robustness to sensor errors, especially those resulting in phantom topography (e.g., omega effects); multiple apparent topographic feature alignments, a situation that is common in areas with few significant features; and numeric instabilities associated with solving problems of this size.

4. The sonar data necessary for these experiments were created by combining actual seafloor depth measurements with a sonar signal synthesizer. The sonar signal generator was taken from a model given by Okino and Higashi [14].

2.3.6 Interferometric Sidescan Sonar Data Processing

Interferometric sidescan sonar swath bathymetry has the advantages of low-cost, simple design, and wide swaths that make it an attractive alternative to multibeam bathymetry systems. However, the simplicity of the physical system is offset by the complexity of the processing required to extract accurate bathymetry from reflected acoustic signals. If interferometric sonar is to produce a reliable bathymetric product that competes favorably with multibeam data, large improvements in the processing stream must occur. These improvements must be implemented at all stages of the production process, from raw data processing to fusion with other bathymetric data sources. In addition to the problems shared with multibeam systems that we have addressed elsewhere in this report, we have identified for future research several areas that are unique to interferometric systems, as described below.

Optimal Phase Recovery. Bathymetry is recovered from phase in an interferometric system. Unfortunately, phase is a random process influenced by multiple factors. Some attempt should be made to apply optimal estimation techniques to the phase recovery problem.

Standard Processing Sequence. Because interferometric systems are just now emerging from the research stage, no production processing sequence has yet been developed. A standard approach, drawn from lessons learned in the multibeam bathymetry field, should be developed.

Beam Sharpening. Sidescan sonar is subject to the blurring effects of beam patterns. These effects can be reduced in radiometric images by deconvolution. Studies should be conducted to determine if similar techniques can be applied to bathymetric data.

SVP Error Reduction. Interferometric bathymetry is very sensitive to changes in sound velocity profile (SVP), requiring frequent recalibration on flat bottom. Techniques that reduce the frequency of recalibration or ameliorate the effects of rapidly changing conditions would greatly improve the quality of data.

3 CONCLUSIONS

The outlier detection software was successfully integrated with the bathymetric production system at NAVOCEANO, where it is now used routinely. The outlier detection algorithm improvements recommended under our earlier program were also implemented, and a preliminary evaluation was carried out. Based on these tests, the primary goal of improving outlier detection performance near regions of significant topographic features appears to have been met. An extensive performance evaluation using human experts as a control, however, was not part of this program.

The feasibility studies carried out under this effort indicate that a significant body of ideas and algorithms is available from existing computer vision and surveillance data analysis systems. Problems such as data fusion, data alignment, and object/feature recognition have already been successfully addressed for these applications. Additional research and a significant amount of engineering will be required before advanced techniques of this kind can be incorporated into oceanographic data production systems.

To gain perspective in the feasibility study on the interactions and prerequisites for oceanographic data processing, a generic data processing block diagram was developed around the requirements put forth by the DHI program. As shown in Figure 11, the overall system comprises three levels: *Sonar Processing*, which includes depth estimation and shipboard navigation; *Data Conditioning and Assessment*, which performs data editing (outlier removal, etc.), renavigation, and quality assessment; and *Product Generation*, which creates the finished data products; i.e., high-level data fusion to support geophysical sciences, provincing/classification for ocean engineering and geomorphological studies, shape recognition to create feature databases and locate potential hazards to navigation, and low-level fusion and gridding to create bathymetric/hydrographic map products. Our investigations found that few of the processing functions outlined in Figure 11 currently exist; of those shown, only the data editing and data gridding blocks have been developed and standardized[5] for the oceanographic community.

Table 3 summarizes the processing technologies that will be required to support the DHI data production capabilities. Note that each of the desired capabilities will require the support of several processing technologies, and conversely (and perhaps more importantly), each processing technology will also be useful to several application areas. We also believe that the development of processing technologies will be expensive, and care must be taken to reduce the redundancy of future R&D efforts that involve them.

5. A standardization effort for gridding algorithms is currently under way.

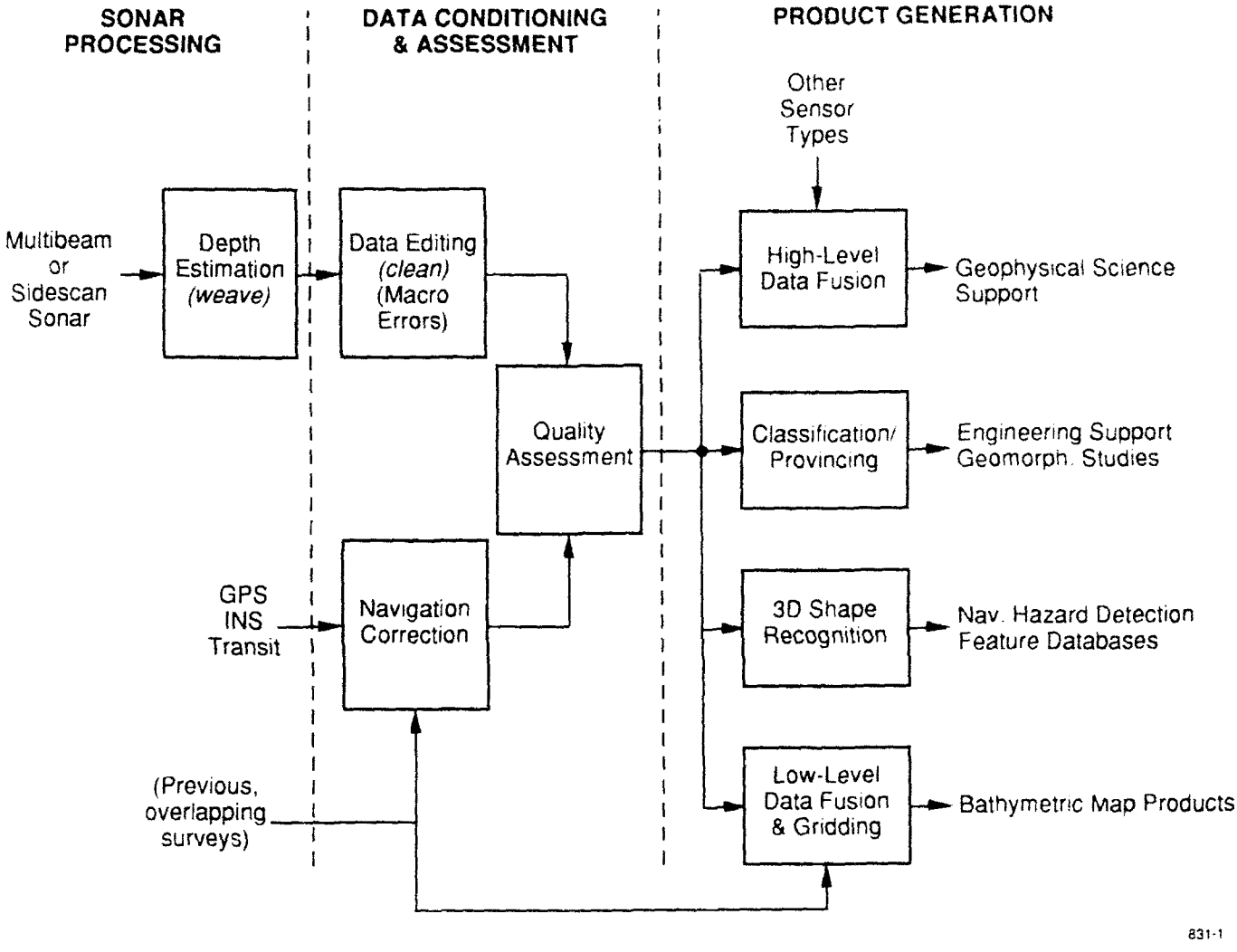

FIGURE 11 GENERIC BATHYMETRIC DATA REDUCTION MODEL

Table 3. TECHNOLOGY REQUIREMENTS MATRIX

Data Production Capabilities \ Core Technologies	Sensor Modeling	3-D Recog-nition	Hypoth. Search	Stat. Image Proc.	Surface Recon-struction	Feature Extraction	Segmen-tation	Nav. Correction/ Registration
Macro Error Detection	●	●	●					
Outlier Error Detection	●			●	●			
Navigational Hazard	●	●		●	●			
Provincing						●	●	
Topo. Classification		●	●			●	●	
Bath/Data Fusion	●		●	●	●			●
Bath/Radiometric Fusion	●	●	●	●	●	●	●	●
Geophysical Interpretation	●	●	●	●	●	●	●	●
Sonar Error Reduction	●			●	●			
Interferometric SS Sonar	●		●	●				

831-2

For these reasons, we believe that the most cost-effective approach to achieving the DHI goals is to identify and develop critical core processing technologies, and then to integrate these into each of the application areas. Each core technology should be developed under a single R&D program; a set of programs could then address each of the specific application areas. For example, a single shape-recognition R&D program could develop the tools necessary for macroscopic error detection and topographic classification. Similarly, a single navigational correction capability could be developed to support the several forms of data fusion, as well as to achieve more precise surveys.

A final point regards the benefits of involving the end-users in the system design process. Especially as DMA begins to focus on more sophisticated processing technology, the required expertise in the diverse areas of oceanography and processing are unlikely to be represented in any one individual. To counter this problem, the algorithm/software experts must work closely with the oceanographers during the design stages. Furthermore, a prototye-and-iterate approach is recommended. In such an approach, a low-cost software prototype is delivered to user facilities prior to the final software product design, evaluated by experts, and then design modifications are made. Although adding slightly to the development cost, this approach insures that the software addresses the user community's needs and, in the long run, better meets the intended goal of improved data analysis efficiency.

REFERENCES

[1] J. Arnold and S. Shaw, "Oceanographic Data Processing Feasibility Study," Technical Research Memorandum for Contract N00014-92-C-0015, SRI Project 3047, SRI International, Menlo Park, CA 94025 (February 1993).

[2] J. Arnold and S. Shaw, "Automated Bathymetric Error Detection Study," Final Report for Contract N00014-90-C-0132, SRI Project 1233, SRI International, Menlo Park, CA 94025 (April 1991).

[3] C. Fox and D. Hayes, "Quantitative Methods for Analyzing the Roughness of the Seafloor," *Reviews of Geophysics*, Vol. 23, No. 1. (February 1985).

[4] A. Blake and A. Zisserman, *Visual Reconstruction*, MIT Press, Cambridge, MA (1987).

[5] R. Kashyap and K. Eom, "Robust Image Modeling Techniques with an Image Restoration Application," *IEEE Transactions on Acoustics, Speech and Signal Processing*, Vol. 36, No. 8 (August 1988).

[6] R. Martin and D. Thompson, "Robust-Resistant Spectrum Estimation," *Proc. IEEE (September 1982).*

[7] S. L. Marple, Jr., *Digital Spectral Analysis with Applications*, Prentice-Hall, Englewood Cliffs, NJ (1987), pp. 397-400.

[8] J. Arnold, "*Clean* System Functional Description," Technical Research Memorandum for Contract N00014-92-C-0015, SRI Project 3047, SRI International, Menlo Park, CA 94025 (July 1992).

[9] J. Arnold, "*Clean* Subsystem Specification," Technical Research Memorandum for Contract N00014-92-C-0015, SRI Project 3047, SRI International, Menlo Park, CA 94025 (August 1992).

[10] J. Arnold, "*Clean* User's Guide," Technical Research Memorandum for Contract N00014-92-C-0015, SRI Project 3047, SRI International, Menlo Park, CA 94025 (September 1992).

[11] C. de Moustier and M. Kleinrock, "Bathymetric Artifacts in Sea Beam Data: How to Recognize Them and What Causes Them," *Journal of Geophysical Research*, Vol. 91, No. B3 (March 1986).

[12] A. Amini, T. Weymouth, and R. Jain, "Using Dynamic Programming for Solving Variational Problems in Vision," *IEEE Trans. on Pattern Analysis,* Vol. 12, No. 6 (September 1990).

[13] A. Amini, T. Weymouth, B. Schunck, and R. Jain, "Surface Weaving with Deformable Signals Based on Dynamic Programming," Technical Report of the Department of Diagnostic Radiology and Electrical Engineering, Yale University (1991).

[14] M. Okino, and Y. Higashi, "Measurement of Seabed Topography by Multibeam Sonar Using CFFT," *IEEE Journal of Ocean Engineering*, Vol. OE-11, No. 4 (October 1986).

[15] C. Nishimura, and D. Forsyth, "Improvements in Navigation Using Seabeam Crossing Errors," *Marine Geophysical Research*, Vol. 9 (1988).

[16] B. Kamgar-Parsi, L. Rosenblum, F. Pipitone, L. Davis, and J. Jones, "Toward an Automated System for a Correctly Registered Bathymetric Chart," *IEEE Journal of Oceanic Engineering,* Vol. 14, No. 4 (October 1989).

[17] B. Kamgar-Parsi, J.L. Jones, and A. Rosenfeld, "Registration of Multiple Overlapping Range Images: Scenes Without Distinctive Features," *IEEE Trans. on Pattern Analysis and Machine Intelligence*, Vol. 13, No. 9 (September 1991).